

# Measurement of single-spin azimuthal asymmetries in semi-inclusive electroproduction of pions and kaons on a longitudinally polarised deuterium target

A. Airapetian,<sup>33</sup> N. Akopov,<sup>33</sup> Z. Akopov,<sup>33</sup> M. Amarian,<sup>7,33</sup> V.V. Ammosov,<sup>25</sup> A. Andrus,<sup>16</sup> E.C. Aschenauer,<sup>7</sup> W. Augustyniak,<sup>32</sup> R. Avakian,<sup>33</sup> A. Avetissian,<sup>33</sup> E. Avetissian,<sup>11</sup> P. Bailey,<sup>16</sup> V. Baturin,<sup>24</sup> C. Baumgarten,<sup>22</sup> M. Beckmann,<sup>6</sup> S. Belostotski,<sup>24</sup> S. Bernreuther,<sup>30</sup> N. Bianchi,<sup>11</sup> H.P. Blok,<sup>23,31</sup> H. Böttcher,<sup>7</sup> A. Borissov,<sup>20</sup> M. Bouwhuis,<sup>16</sup> J. Brack,<sup>5</sup> A. Brüll,<sup>19</sup> V. Bryzgalov,<sup>25</sup> G.P. Capitani,<sup>11</sup> H.C. Chiang,<sup>16</sup> G. Ciullo,<sup>10</sup> M. Contalbrigo,<sup>10</sup> G.R. Court,<sup>17</sup> P.F. Dalpiaz,<sup>10</sup> R. De Leo,<sup>3</sup> L. De Nardo,<sup>1</sup> E. De Sanctis,<sup>11</sup> E. Devitsin,<sup>21</sup> P. Di Nezza,<sup>11</sup> M. Düren,<sup>14</sup> M. Ehrenfried,<sup>9</sup> A. Elalaoui-Moulay,<sup>2</sup> G. Elbakian,<sup>33</sup> F. Ellinghaus,<sup>7</sup> U. Elschenbroich,<sup>13</sup> J. Ely,<sup>5</sup> R. Fabbri,<sup>10</sup> A. Fantoni,<sup>11</sup> A. Fechtchenko,<sup>8</sup> L. Felawka,<sup>29</sup> B. Fox,<sup>5</sup> J. Franz,<sup>12</sup> S. Frullani,<sup>27</sup> Y. Gärber,<sup>9</sup> G. Gapienko,<sup>25</sup> V. Gapienko,<sup>25</sup> F. Garibaldi,<sup>27</sup> E. Garutti,<sup>23</sup> D. Gaskell,<sup>5</sup> G. Gavrillov,<sup>24</sup> V. Gharibyan,<sup>33</sup> G. Graw,<sup>22</sup> O. Grebeniuk,<sup>24</sup> L.G. Greeniaus,<sup>1,29</sup> W. Haeberli,<sup>18</sup> K. Hafidi,<sup>2</sup> M. Hartig,<sup>29</sup> D. Hasch,<sup>11</sup> D. Heesbeen,<sup>23</sup> M. Henoeh,<sup>9</sup> R. Hertenberger,<sup>22</sup> W.H.A. Hesselink,<sup>23,31</sup> A. Hillenbrand,<sup>9</sup> Y. Holler,<sup>6</sup> B. Hommez,<sup>13</sup> G. Iarygin,<sup>8</sup> A. Ivanilov,<sup>25</sup> A. Izotov,<sup>24</sup> H.E. Jackson,<sup>2</sup> A. Jgoun,<sup>24</sup> R. Kaiser,<sup>15</sup> E. Kinney,<sup>5</sup> A. Kisselev,<sup>24</sup> K. Königsmann,<sup>12</sup> H. Kolster,<sup>19</sup> M. Kopytin,<sup>24</sup> V. Korotkov,<sup>7,25</sup> V. Kozlov,<sup>21</sup> B. Krauss,<sup>9</sup> V.G. Krivokhijine,<sup>8</sup> L. Lagamba,<sup>3</sup> L. Lapikás,<sup>23</sup> A. Laziev,<sup>23,31</sup> P. Lenisa,<sup>10</sup> P. Liebing,<sup>7</sup> T. Lindemann,<sup>6</sup> K. Lipka,<sup>7</sup> W. Lorenzon,<sup>20</sup> B.-Q. Ma,<sup>4</sup> N.C.R. Makins,<sup>16</sup> H. Marukyan,<sup>33</sup> F. Masoli,<sup>10</sup> F. Menden,<sup>12</sup> V. Mexner,<sup>23</sup> N. Meyners,<sup>6</sup> O. Mikloukho,<sup>24</sup> C.A. Miller,<sup>1,29</sup> Y. Miyachi,<sup>30</sup> V. Muccifora,<sup>11</sup> A. Nagaitsev,<sup>8</sup> E. Nappi,<sup>3</sup> Y. Naryshkin,<sup>24</sup> A. Nass,<sup>9</sup> W.-D. Nowak,<sup>7</sup> K. Oganessyan,<sup>6,11</sup> H. Ohsuga,<sup>30</sup> G. Orlandi,<sup>27</sup> S. Potashov,<sup>21</sup> D.H. Potterveld,<sup>2</sup> M. Raithel,<sup>9</sup> D. Reggiani,<sup>10</sup> P.E. Reimer,<sup>2</sup> A. Reischl,<sup>23</sup> A.R. Reolon,<sup>11</sup> K. Rith,<sup>9</sup> G. Rosner,<sup>15</sup> A. Rostomyan,<sup>33</sup> D. Ryckbosch,<sup>13</sup> I. Sanjiev,<sup>2,24</sup> I. Savin,<sup>8</sup> C. Scarlett,<sup>20</sup> A. Schäfer,<sup>26</sup> C. Schill,<sup>11,12</sup> G. Schnell,<sup>7</sup> K.P. Schüler,<sup>6</sup> A. Schwind,<sup>7</sup> R. Seidl,<sup>9</sup> J. Seibert,<sup>12</sup> B. Seitz,<sup>1</sup> R. Shandize,<sup>9</sup> T.-A. Shibata,<sup>30</sup> V. Shutov,<sup>8</sup> M.C. Simani,<sup>23,31</sup> K. Sinram,<sup>6</sup> M. Stancari,<sup>10</sup> M. Statera,<sup>10</sup> E. Steffens,<sup>9</sup> J.J.M. Steijger,<sup>23</sup> J. Stewart,<sup>7</sup> U. Stösslein,<sup>5</sup> H. Tanaka,<sup>30</sup> S. Taroian,<sup>33</sup> B. Tchuiko,<sup>25</sup> A. Terkulov,<sup>21</sup> S. Tessarin,<sup>22</sup> E. Thomas,<sup>11</sup> A. Tkabladze,<sup>7</sup> A. Trzcinski,<sup>32</sup> M. Tytgat,<sup>13</sup> G.M. Urciuoli,<sup>27</sup> P. van der Nat,<sup>23</sup> G. van der Steenhoven,<sup>23</sup> R. van de Vyver,<sup>13</sup> M.C. Vetterli,<sup>28,29</sup> V. Vikhrov,<sup>24</sup> M.G. Vinciter,<sup>1</sup> J. Visser,<sup>23</sup> C. Vogel,<sup>9</sup> M. Vogt,<sup>9</sup> J. Volmer,<sup>7</sup> C. Weiskopf,<sup>9</sup> J. Wendland,<sup>28,29</sup> J. Wilbert,<sup>9</sup> T. Wise,<sup>18</sup> S. Yen,<sup>29</sup> S. Yoneyama,<sup>30</sup> B. Zihlmann,<sup>23</sup> H. Zohrabian,<sup>33</sup> and P. Zupranski<sup>32</sup>

(The HERMES Collaboration)

<sup>1</sup>Department of Physics, University of Alberta, Edmonton, Alberta T6G 2J1, Canada

<sup>2</sup>Physics Division, Argonne National Laboratory, Argonne, Illinois 60439-4843, USA

<sup>3</sup>Istituto Nazionale di Fisica Nucleare, Sezione di Bari, 70124 Bari, Italy

<sup>4</sup>Department of Physics, Peking University, Beijing 100871, China

<sup>5</sup>Nuclear Physics Laboratory, University of Colorado, Boulder, Colorado 80309-0446, USA

<sup>6</sup>DESY, Deutsches Elektronen-Synchrotron, 22603 Hamburg, Germany

<sup>7</sup>DESY Zeuthen, 15738 Zeuthen, Germany

<sup>8</sup>Joint Institute for Nuclear Research, 141980 Dubna, Russia

<sup>9</sup>Physikalisches Institut, Universität Erlangen-Nürnberg, 91058 Erlangen, Germany

<sup>10</sup>Istituto Nazionale di Fisica Nucleare, Sezione di Ferrara and

Dipartimento di Fisica, Università di Ferrara, 44100 Ferrara, Italy

<sup>11</sup>Istituto Nazionale di Fisica Nucleare, Laboratori Nazionali di Frascati, 00044 Frascati, Italy

<sup>12</sup>Fakultät für Physik, Universität Freiburg, 79104 Freiburg, Germany

<sup>13</sup>Department of Subatomic and Radiation Physics, University of Gent, 9000 Gent, Belgium

<sup>14</sup>Physikalisches Institut, Universität Gießen, 35392 Gießen, Germany

<sup>15</sup>Department of Physics and Astronomy, University of Glasgow, Glasgow G12 8QQ, United Kingdom

<sup>16</sup>Department of Physics, University of Illinois, Urbana, Illinois 61801, USA

<sup>17</sup>Physics Department, University of Liverpool, Liverpool L69 7ZE, United Kingdom

<sup>18</sup>Department of Physics, University of Wisconsin-Madison, Madison, Wisconsin 53706, USA

<sup>19</sup>Laboratory for Nuclear Science, Massachusetts Institute of Technology, Cambridge, Massachusetts 02139, USA

<sup>20</sup>Randall Laboratory of Physics, University of Michigan, Ann Arbor, Michigan 48109-1120, USA

<sup>21</sup>Lebedev Physical Institute, 117924 Moscow, Russia

<sup>22</sup>Sektion Physik, Universität München, 85748 Garching, Germany

<sup>23</sup>Nationaal Instituut voor Kernfysica en Hoge-Energiefysica (NIKHEF), 1009 DB Amsterdam, The Netherlands

<sup>24</sup>Petersburg Nuclear Physics Institute, St. Petersburg, Gatchina, 188350 Russia

<sup>25</sup>Institute for High Energy Physics, Protvino, Moscow region, 142284 Russia

<sup>26</sup>Institut für Theoretische Physik, Universität Regensburg, 93040 Regensburg, Germany

<sup>27</sup>Istituto Nazionale di Fisica Nucleare, Sezione Roma 1, Gruppo Sanità and Physics Laboratory, Istituto Superiore di Sanità, 00161 Roma, Italy

<sup>28</sup>*Department of Physics, Simon Fraser University, Burnaby, British Columbia V5A 1S6, Canada*

<sup>29</sup>*TRIUMF, Vancouver, British Columbia V6T 2A3, Canada*

<sup>30</sup>*Department of Physics, Tokyo Institute of Technology, Tokyo 152, Japan*

<sup>31</sup>*Department of Physics and Astronomy, Vrije Universiteit, 1081 HV Amsterdam, The Netherlands*

<sup>32</sup>*Andrzej Soltan Institute for Nuclear Studies, 00-689 Warsaw, Poland*

<sup>33</sup>*Yerevan Physics Institute, 375036 Yerevan, Armenia*

(Dated: May 21, 2019)

Single-spin asymmetries have been measured for semi-inclusive electroproduction of  $\pi^+$ ,  $\pi^-$ ,  $\pi^0$  and  $K^+$  mesons in deep-inelastic scattering off a longitudinally polarised deuterium target. The asymmetries appear in the distribution of the hadrons in the azimuthal angle  $\phi$  around the virtual photon direction, relative to the lepton scattering plane. The corresponding analysing powers in the  $\sin\phi$  moment of the cross section are  $0.012 \pm 0.002(\text{stat.}) \pm 0.002(\text{syst.})$  for  $\pi^+$ ,  $0.006 \pm 0.003(\text{stat.}) \pm 0.002(\text{syst.})$  for  $\pi^-$ ,  $0.021 \pm 0.005(\text{stat.}) \pm 0.003(\text{syst.})$  for  $\pi^0$  and  $0.013 \pm 0.006(\text{stat.}) \pm 0.003(\text{syst.})$  for  $K^+$ . The  $\sin 2\phi$  moments are compatible with zero for all particles.

PACS numbers: 13.87.Fh, 13.60.-r, 13.88.+e, 14.20.Dh

Deep-inelastic lepton scattering (DIS) on polarised nucleons has provided much of our present understanding of the spin structure of the nucleon. Recently, measurements of single-spin azimuthal asymmetries have been recognised as a powerful source of information about the spin structure of the nucleon [1], complementary to inclusive deep-inelastic scattering. Significant azimuthal target-spin asymmetries in electroproduction of  $\pi^+$  and  $\pi^0$  mesons on a longitudinally polarised hydrogen target have been reported in Refs. [2, 3]. Evidence for azimuthal asymmetries of pions has also been reported for deep-inelastic lepton scattering off transversely polarised protons [4].

It has been suggested [5] that these single-spin asymmetries may provide information on the transversity distribution, which describes in a transverse polarisation basis the probability to find a quark with its spin parallel or antiparallel to the spin of the nucleon that is polarised transversely to its (infinite) momentum [6, 7, 8]. Transversity is a chiral-odd distribution function, which implies that it is not observable in an inclusive measurement, because chirality is conserved in electromagnetic and strong interactions in the limit of massless on-shell quarks. Therefore, a second chiral-odd object has to be involved in the process [9, 10]. In semi-inclusive scattering this can be a chiral-odd fragmentation function — for example the Collins-function [5].

The HERMES results on target single-spin asymmetries [2, 3] have elicited a number of phenomenological studies to evaluate these asymmetries in the framework of the Collins mechanism using various models as input for the chiral-odd distribution and fragmentation functions [11, 12, 13, 14, 15, 16, 17, 18, 19, 20, 21]. Theoretical predictions have also been made for single-spin asymmetries in DIS off the nucleons in a deuterium target [21, 22].

Recently, it has been shown that another mechanism can also cause a single-spin azimuthal asymmetry in semi-inclusive deep-inelastic scattering [23]. In this case, the observed asymmetry is attributed to the interaction

of the struck quark with the target remnant through the exchange of a single gluon. This mechanism was shown to be identical [24] to the Sivers effect known already for a long time [25], involving a chiral-even time-odd distribution function. Other theoretical studies [26, 27, 28, 29] have revealed that factorisation applies to this process, which leads to gauge-invariant momentum dependent parton distributions.

Experimentally, Collins and Sivers mechanism can be distinguished when scattering on a transversely polarised target. In this case, the two mechanisms show a different dependence on the azimuthal angle  $\phi_s$  of the target spin vector around the virtual photon direction with respect to the lepton scattering plane. While for the Collins effect the relevant angular dependence of the cross section is  $\sin(\phi + \phi_s)$ , the Sivers effect is characterised by a  $\sin(\phi - \phi_s)$  moment [30]. Here,  $\phi$  is the azimuthal angle of the scattered meson around the virtual photon direction with respect to the lepton scattering plane (see Fig. 1). In the case of a longitudinally polarised target  $\phi_s$  is zero or  $\pi$  and the two mechanisms cannot be distinguished. However, for the two mechanisms a different kinematic dependence on the fractional energy  $z$  of the hadron has been predicted [29].

This paper reports the first observation of target-spin azimuthal asymmetries for semi-inclusive pion and kaon production on a longitudinally polarised deuterium target. The data were recorded during the 1998, 1999 and 2000 running periods of the HERMES experiment. The experiment was performed with a beam of 27.6 GeV polarised electrons/positrons from the HERA storage ring at DESY and polarised nucleons in a deuterium gas target. The average target polarisation was 0.84 with a fractional uncertainty of 5%. The data were taken with an electron beam in 1998 and with a positron beam in 1999 and 2000. The measured single-spin asymmetries show no dependence on the beam charge. Therefore, all datasets were combined. In the following, electrons and positrons will be jointly referred to as positrons.

The process considered is the production of a pseu-

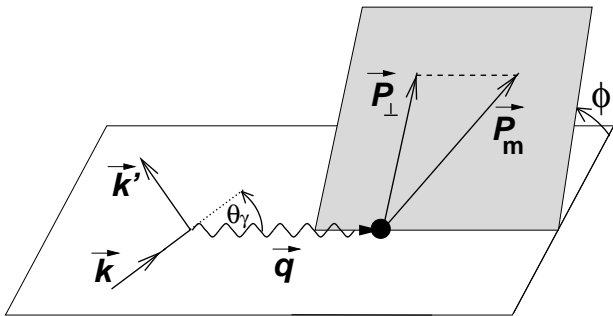


FIG. 1: Kinematic planes for meson production in semi-inclusive deep-inelastic scattering: Lepton scattering plane (*white*) and the meson production plane (*shaded*).

doscalar meson ( $m = \pi$  or  $K$ ) in deep-inelastic positron scattering off a longitudinally polarised deuterium target:

$$e + \vec{d} \rightarrow e + m + X. \quad (1)$$

The kinematics of this scattering process are illustrated in Fig. 1. The relevant variables are the squared four-momentum  $-Q^2 = q^2 = (k - k')^2$  and the energy  $\nu = E - E'$  of the virtual photon in the target rest frame and its fractional energy  $y = \nu/E$ , the invariant mass of the virtual-photon nucleon system  $W = \sqrt{2M\nu + M^2 - Q^2}$ , the Bjorken variable  $x = Q^2/2M\nu$  and the fractional energy  $z = E_m/\nu$  of the produced meson. Here,  $k$  ( $k'$ ) and  $E$  ( $E'$ ) are the 4-momenta and the energies of the incident (scattered) positron and  $M$  is the nucleon mass. The energy and momentum of the meson in the target rest frame are given by  $E_m$  and  $P_m$ , respectively. The transverse momentum  $P_\perp$  of the produced meson is defined with respect to the virtual-photon direction. The magnitude of the azimuthal angle  $\phi$  of the scattered meson is evaluated by

$$\cos \phi = \frac{(\vec{q} \times \vec{k}) \cdot (\vec{q} \times \vec{P}_m)}{|\vec{q} \times \vec{k}| |\vec{q} \times \vec{P}_m|} \quad (2)$$

and its sign by  $(\vec{q} \times \vec{k}) \cdot \vec{P}_m / |(\vec{q} \times \vec{k}) \cdot \vec{P}_m|$ . In the case of a target polarised longitudinally with respect to the incident positron direction, the target polarisation vector has components parallel and orthogonal with respect to the virtual photon. The longitudinal and the transverse component of the target polarisation vector are given by  $\cos \theta_\gamma$  and  $\sin \theta_\gamma$ , respectively. Here,  $\theta_\gamma$  is the angle between the incident positron and the virtual photon in the photon-nucleon centre-of-mass system. In the HERMES acceptance, the mean values of  $\langle \cos \theta_\gamma \rangle$  and  $\langle \sin \theta_\gamma \rangle$  are 0.98 and 0.16, respectively.

For the measurement of a single target-spin asymmetry the positron beam has to be unpolarised. The

positrons in the HERA storage ring are naturally transversely polarised by the emission of synchrotron radiation [31]. The transverse polarisation is transformed into longitudinal polarisation and back to transverse polarisation by two spin-rotators [32] upstream and downstream of the HERMES experiment, respectively. The sign of the beam polarisation is changed about every two months, which requires moving the magnets of the spin rotators and inverting their magnetic field direction. The transverse and the longitudinal positron polarisation are continuously monitored by two Compton-backscattering polarimeters [33, 34]. To obtain an unpolarised beam, a polarisation and luminosity weighted average is formed from data of periods with opposite beam spin orientations. The averaged luminosity weighted beam polarisation in the analysed data sample is  $0.0\% \pm 0.1\%(\text{stat.}) \pm 2.0\%(\text{syst.})$ .

The scattered positrons and associated mesons are detected by the HERMES spectrometer [35] in the range  $0.04 \text{ rad} < \theta < 0.22 \text{ rad}$  of the polar angle. Positron and hadron separation is based on the information from four detectors: a transition-radiation detector, a dual radiator ring imaging Čerenkov detector (RICH) [36], a preshower scintillation detector and a lead-glass electromagnetic calorimeter [37]. This system provides an average positron identification efficiency of 98% with a hadron contamination below 1%.

Events are required to contain only one electron or positron track with the same charge as the beam particle and in addition at least one meson. If more than one meson is detected in the spectrometer, only the meson with the largest momentum is considered. Identification of charged pions or kaons in the momentum range  $2 \text{ GeV} < P_m < 15 \text{ GeV}$  is accomplished using the information from the RICH. Based on a Monte Carlo simulation of the RICH, detection efficiencies for charged pions or kaons are determined as a function of the hadron momentum and the hadron multiplicity. The average identification efficiency in the RICH is 97% for pions and 88% for kaons. The detection efficiencies are used to unfold the true hadron populations from the measured ones.

Neutral pions are identified by the detection of two photons in the electromagnetic calorimeter. The reconstructed energy for each photon is required to be at least 1.0 GeV and each photon hit in the calorimeter is required not to be associated with any charged particle track going in the same direction. The reconstructed photon-pair invariant mass  $M_{\gamma\gamma}$  distribution shows a clear  $\pi^0$  mass peak with a mass resolution of about 0.012 GeV, as displayed in Fig. 2. Neutral pions are selected within the invariant mass range  $0.10 \text{ GeV} < M_{\gamma\gamma} < 0.17 \text{ GeV}$ . The background contribution from uncorrelated photons to the reconstructed invariant mass spectrum decreases with increasing  $z$  of the hadron and ranges from 35% for the lowest  $z$  bin to less than 5% for the highest bin. The asymmetry of this background is de-

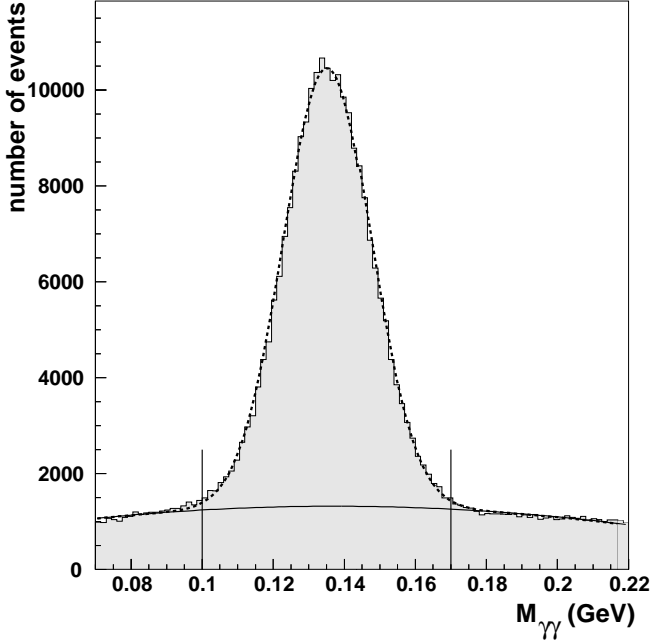


FIG. 2: Invariant mass ( $M_{\gamma\gamma}$ ) spectrum of photon pairs measured in the electromagnetic calorimeter. A fit to the data using a Gaussian function for the peak plus a second order polynomial (solid curve) for the background of uncorrelated photons is shown as the dotted curve. The two vertical lines embrace the invariant mass interval used for  $\pi^0$  identification.

terminated outside of the mass window of the  $\pi^0$  mass peak and is found to be compatible with zero. A correction is applied to account for this dilution.

The requirements imposed on the kinematics of the scattered positron are the same as those in the previous analyses of the hydrogen data [2, 3]:  $1 \text{ GeV}^2 < Q^2 < 15 \text{ GeV}^2$ ,  $W > 2 \text{ GeV}$ ,  $0.023 < x < 0.4$  and  $y < 0.85$ . Contributions from target fragmentation are suppressed by requiring  $z > 0.2$  and exclusive meson production is suppressed by the cut  $z < 0.7$ . A lower limit of 50 MeV is imposed on  $P_{\perp}$  to ensure an accurate measurement of the azimuthal angle  $\phi$ .

The target-spin asymmetry  $A_{UL}$  in the cross section of scattering an unpolarised beam (U) on a longitudinally polarised target (L) is evaluated as

$$A_{UL}(\phi) = \frac{1}{|P_L|} \cdot \frac{N^{\rightarrow}(\phi)/L^{\rightarrow} - N^{\leftarrow}(\phi)/L^{\leftarrow}}{N^{\rightarrow}(\phi)/L^{\rightarrow} + N^{\leftarrow}(\phi)/L^{\leftarrow}}, \quad (3)$$

where  $N^{\rightarrow(\leftarrow)}$  is the number of pions or kaons detected for target spin antiparallel (parallel) to direction of the beam momentum,  $L^{\rightarrow(\leftarrow)}$  is the respective dead-time corrected luminosity, and  $P_L$  the average longitudinal target polarisation. The asymmetry for  $\pi^0$  mesons is corrected for the dilution from the background of uncorrelated photons using the equation

$$A_{\text{corr}}(\phi) = \frac{N_{\pi^0} + N_{\text{bg}}}{N_{\pi^0}} \cdot A_{\text{meas}}(\phi) - \frac{N_{\text{bg}}}{N_{\pi^0}} \cdot A_{\text{bg}}(\phi). \quad (4)$$

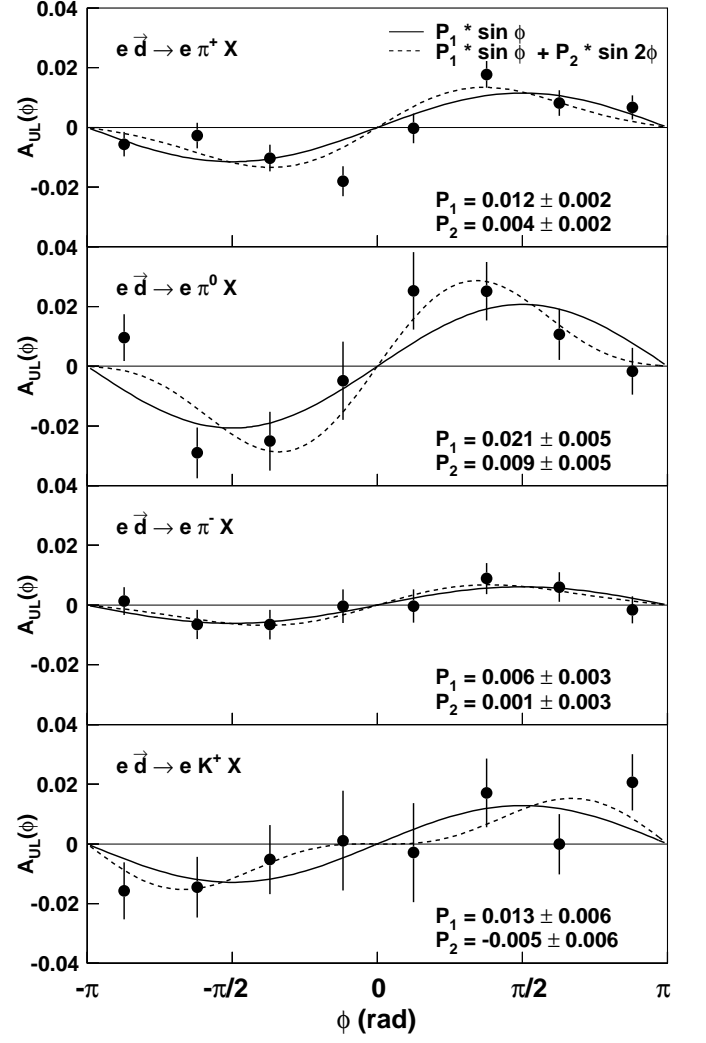


FIG. 3: Target spin asymmetries  $A_{UL}(\phi)$  for electroproduction of  $\pi^+$ ,  $\pi^0$ ,  $\pi^-$  and  $K^+$  mesons. Fits to the form  $P_0 + P_1 \sin \phi$  (solid line) and  $P_0 + P_1 \sin \phi + P_2 \sin 2\phi$  (dashed line) are also displayed in the figure. The error bars give the statistical uncertainties of the measurements. The values of the coefficients  $P_0$  are all compatible with zero and the coefficients  $P_1$  and  $P_2$  for the various hadrons and their statistical uncertainties are listed in each panel.

Here  $N_{\pi^0}$  and  $N_{\text{bg}}$  are the number of neutral pions and background-photon pairs, respectively, in each kinematic bin. The asymmetries for  $\pi^0$  mesons  $A_{\text{meas}}$  and for the background of uncorrelated photons  $A_{\text{bg}}$  are calculated as defined in Eq. (3). The background asymmetry is found to be consistent with zero.

In Fig. 3, the azimuthal asymmetries  $A_{UL}(\phi)$  for the mesons  $\pi^+$ ,  $\pi^0$ ,  $\pi^-$  and  $K^+$  are displayed as a function of  $\phi$ , integrated over the experimental acceptance in the kinematic variables  $x$ ,  $P_{\perp}$ ,  $z$ ,  $y$  and  $Q^2$ . The average values are  $\langle x \rangle = 0.09$ ,  $\langle P_{\perp} \rangle = 0.40 \text{ GeV}$ ,  $\langle z \rangle = 0.38$ ,  $\langle y \rangle = 0.53$  and  $\langle Q^2 \rangle = 2.4 \text{ GeV}^2$ .

The asymmetries defined in Eq. (3) were alternatively

	meson	deuterium target	proton target [2, 3]
$A_{UL}^{\sin \phi}$	$\pi^+$	$0.012 \pm 0.002 \pm 0.002$	$0.022 \pm 0.005 \pm 0.003$
	$\pi^0$	$0.021 \pm 0.005 \pm 0.003$	$0.019 \pm 0.007 \pm 0.003$
	$\pi^-$	$0.006 \pm 0.003 \pm 0.002$	$-0.002 \pm 0.006 \pm 0.004$
	$K^+$	$0.013 \pm 0.006 \pm 0.003$	—
$A_{UL}^{\sin 2\phi}$	$\pi^+$	$0.004 \pm 0.002 \pm 0.002$	$-0.002 \pm 0.005 \pm 0.003$
	$\pi^0$	$0.009 \pm 0.005 \pm 0.003$	$0.006 \pm 0.007 \pm 0.003$
	$\pi^-$	$0.001 \pm 0.003 \pm 0.002$	$-0.005 \pm 0.006 \pm 0.005$
	$K^+$	$-0.005 \pm 0.006 \pm 0.003$	—

TABLE I: Analysing powers  $A_{UL}^{\sin \phi}$  and  $A_{UL}^{\sin 2\phi}$  for the azimuthal target-spin asymmetry for the electroproduction of pions and kaons on the deuteron, integrated over the experimental acceptance in  $x$ ,  $P_\perp$ ,  $z$ ,  $y$  and  $Q^2$ . Also listed are earlier results obtained on the proton from Ref. [2, 3]. The first uncertainty is the statistical and the second is the systematic uncertainty of the measurement.

fit with the functions

$$f_1(\phi) = P_0 + P_1 \sin \phi \quad (5)$$

$$f_2(\phi) = P_0 + P_1 \sin \phi + P_2 \sin 2\phi, \quad (6)$$

which are indicated as curves in Fig. 3. All coefficients  $P_0$  are compatible with zero. The  $\sin \phi$  and  $\sin 2\phi$  amplitudes  $P_1$  and  $P_2$ , obtained from the fits to the data, are displayed in the figure as well. They represent the analysing powers  $A_{UL}^{\sin \phi}$  and  $A_{UL}^{\sin 2\phi}$  of the azimuthal asymmetry. The numerical values are given in Tab. I for the various mesons, together with the previously reported analysing powers for pion production on longitudinally polarised protons [2, 3].

The effects of smearing and spectrometer acceptance are estimated using a Monte Carlo simulation. For this purpose, a Monte Carlo simulation is carried out with various  $x$ ,  $P_\perp$  or  $z$  dependent  $\sin \phi$  and  $\sin 2\phi$  amplitudes. Within the statistical accuracy, the reconstructed event distributions show the same  $\sin \phi$  and  $\sin 2\phi$  amplitudes as the generated distributions. An example is shown in Fig. 4. It is concluded from the Monte Carlo simulation that the measured asymmetries are not affected by acceptance or smearing effects of the detector in any significant way within the statistical precision of the Monte Carlo simulation of 0.001 (0.002) for charged mesons ( $\pi^0$ ).

An additional test of possible acceptance effects was performed using measurements with unpolarised hydrogen and deuterium gas targets. These measurements were regularly done after a few hours of data taking with polarised targets. The data were analysed with the kinematic requirements described above and the  $\sin \phi$  and  $\sin 2\phi$  moments  $A_{UU}^{\sin \phi}$  and  $A_{UU}^{\sin 2\phi}$  of the unpolarised cross section are extracted. They were calculated respectively as  $A_{UU}^{\sin \phi} = 1/N \sum_{i=1}^N \sin \phi_i$  and  $A_{UU}^{\sin 2\phi} = 1/N \sum_{i=1}^N \sin 2\phi_i$ , summed over all  $N$  events taken with unpolarised target gas. Since these moments are ex-

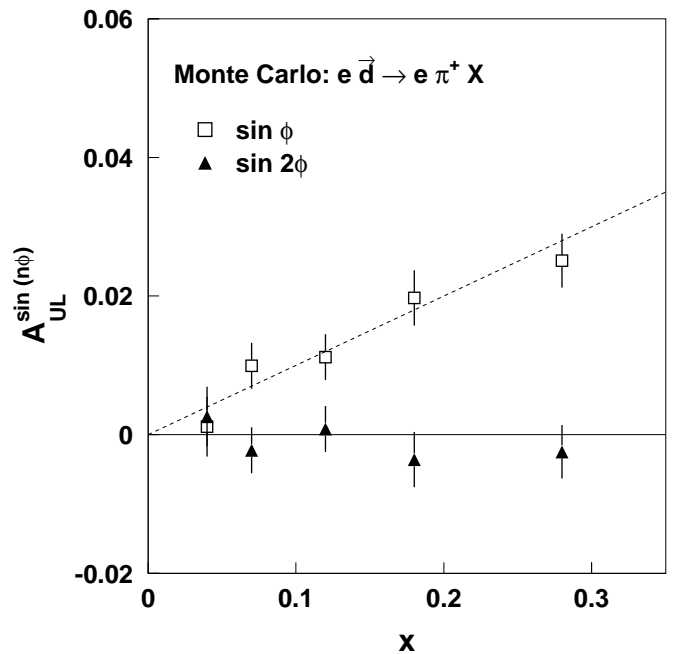


FIG. 4: Analysing powers  $A_{UL}^{\sin \phi}$  (open squares) and  $A_{UL}^{\sin 2\phi}$  (filled triangles) for  $\pi^+$  mesons from a Monte Carlo simulation. An  $x$  dependent azimuthal asymmetry for  $\sin \phi$  (dashed line) and zero for  $\sin 2\phi$  (solid line) has been introduced into the Monte Carlo event generator. The error bars give the statistical uncertainties of the reconstructed Monte Carlo data.

pected to be zero [1], the results constitute upper limits on possible  $\sin \phi$  and  $\sin 2\phi$  moments induced by the detector acceptance. The moments  $A_{UU}^{\sin \phi}$  and  $A_{UU}^{\sin 2\phi}$  were found to be consistent with zero for pions (kaons) within a statistical uncertainty of 0.002 (0.004).

The analysing powers  $A_{UL}^{\sin \phi}$  extracted from a fit to the asymmetry  $A_{UL}(\phi)$  have been compared to those obtained as moments:

$$A_{UL}^W = \frac{1}{|P_L|} \frac{\frac{1}{L^{\rightarrow}} \sum_{i=1}^{N^{\rightarrow}} W(\phi_i) - \frac{1}{L^{\leftarrow}} \sum_{i=1}^{N^{\leftarrow}} W(\phi_i)}{\frac{1}{2} [N^{\rightarrow}/L^{\rightarrow} + N^{\leftarrow}/L^{\leftarrow}]}, \quad (7)$$

using the weighting functions  $W(\phi) = \sin \phi$  and  $W(\phi) = \sin 2\phi$ , respectively. This type of analysis is more sensitive to the experimental acceptance [3]. Based on a Monte Carlo simulation, corrections of about 15% had to be applied to account for a cross-contamination between the  $\sin \phi$  and  $\sin 2\phi$  moments. After these corrections, the analysing powers extracted as moments according to Eq. (7) and those extracted using a fit to the cross section asymmetry  $A_{UL}(\phi)$  agree within the systematic uncertainty assigned to effects of the spectrometer acceptance (see Tab. III).

In Fig. 5, the analysing powers  $A_{UL}^{\sin \phi}$  on the deuteron are shown as a function of  $x$ ,  $P_\perp$  and  $z$  together with earlier results obtained on the proton [2, 3]. The mean values of  $Q^2$  for each  $x$  bin and the mean values of  $P_\perp$

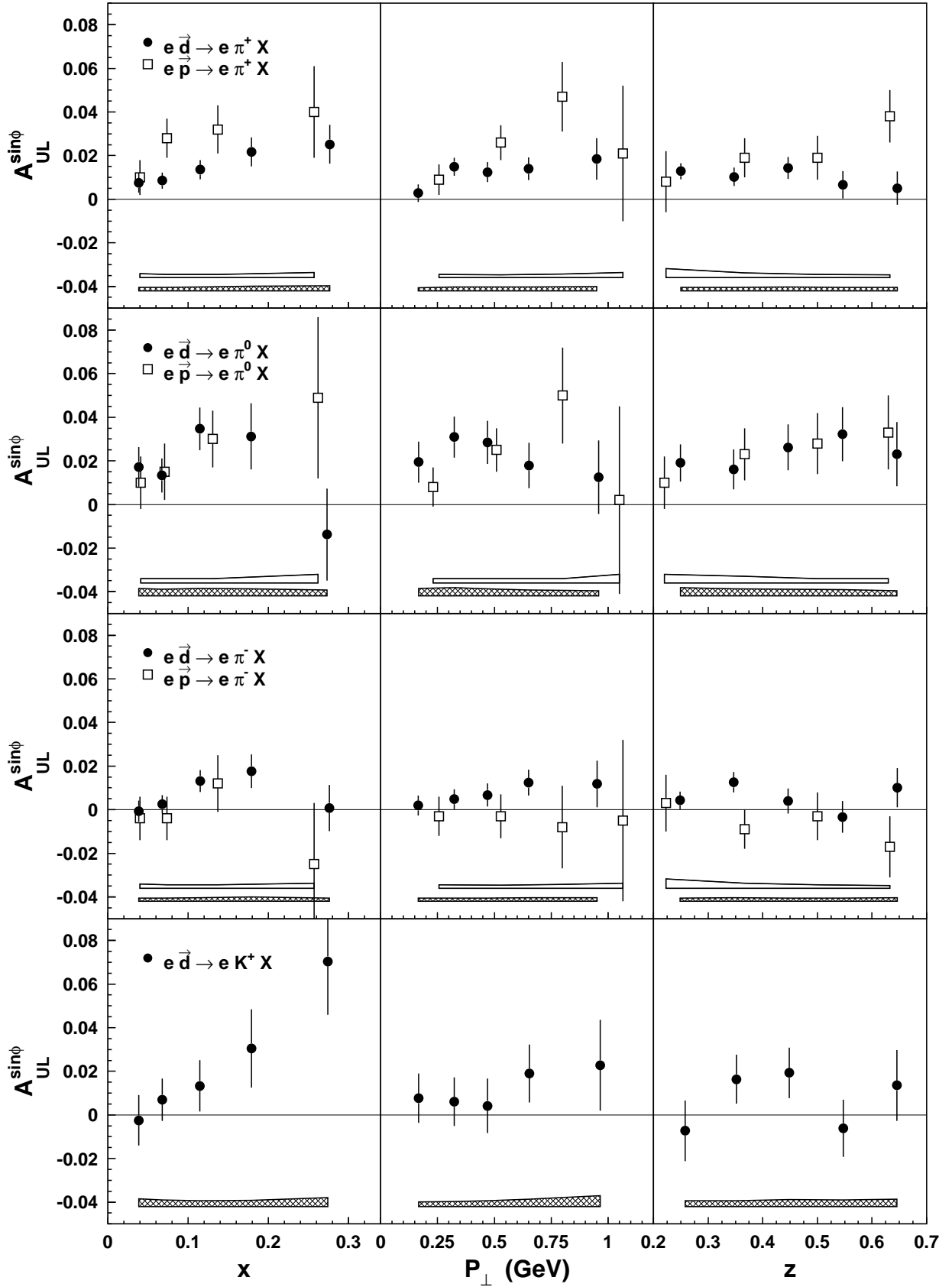


FIG. 5: Target spin analysing powers  $A_{UL}^{\sin\phi}$  for semi-inclusive  $\pi^+$ ,  $\pi^0$ ,  $\pi^-$  and  $K^+$  production on the deuteron (filled circles) and on the proton (open squares). The latter are taken from Refs. [2, 3]. The data are shown as a function of one of the kinematic variables  $x$ ,  $P_{\perp}$  and  $z$  while integrating over the other variables. The error bars give the statistical uncertainties of the measurements and the bands in the lower parts of each panel give the systematic uncertainties for the deuteron (hashed band) and for the proton measurement (open band).

$x$	0.039	0.068	0.115	0.179	0.276
$\langle Q^2 \rangle$ in GeV <sup>2</sup>	1.30	1.82	2.62	3.58	4.88
$z$	0.25	0.35	0.45	0.55	0.65
$\langle P_{\perp} \rangle$ in GeV	0.36	0.40	0.44	0.46	0.47

TABLE II: Mean values of  $Q^2$  for each  $x$  bin (*upper table*) and mean values of  $P_{\perp}$  for each bin of  $z$  (*lower table*).

source of systematic uncertainty	$\pi^+, \pi^-$	$\pi^0$	$K^+$
determination of target polarisation	0.001	0.001	0.001
upper limit on acceptance effects	0.001	0.002	0.001
meson identification (RICH)	0.0004	-	0.002
$\rho^0$ contamination	0.001	-	-
$\gamma\gamma$ -background correction	-	0.002	-
quadratic sum	0.002	0.003	0.003

TABLE III: Contributions to the systematic uncertainty of the experimental results for the target spin analysing powers  $A_{\text{UL}}^{\sin\phi}$  listed in Tab. I for  $\pi^+$ ,  $\pi^-$ ,  $\pi^0$  and  $K^+$  mesons. The total systematic uncertainty is calculated as the quadratic sum of the individual contributions.

for each  $z$  bin are given in Tab. II.

The various contributions to the systematic uncertainty of the experimental results in Tab. I, integrated over  $x$ ,  $P_{\perp}$  and  $z$ , are listed in Tab. III. For charged pions, the largest contributions originate from the determination of the target polarisation and from the upper limit for possible acceptance effects evaluated in a Monte Carlo simulation. For kaons the uncertainty in the hadron identification with the RICH detector also contributes significantly. For pions the RICH efficiency is larger and the contamination by other hadrons is smaller so that the contribution to the systematic uncertainty is small. The contamination of the charged pion sample by pions from the decay of exclusively produced  $\rho^0$  vector mesons is estimated using a Monte Carlo simulation and is found to be smaller than 5%. In addition, it is shown from the experimental data that there is no asymmetry in their azimuthal distribution. A contribution is added to the systematic uncertainty for this dilution. For  $\pi^0$  mesons there is a significant contribution to the systematic uncertainty due to the uncertainty in the determination of the background yield and its asymmetry.

The analysing power  $A_{\text{UL}}^{\sin\phi}$  for  $\pi^+$  production on the deuteron is greater than zero, but smaller than that obtained on the proton (see Tab. I). In the context of models based on transversity, the different size of the asymmetries for  $\pi^+$  production on the proton and deuteron can be attributed to the dominant role of the  $u$ -quark contribution to the observed asymmetry [22]. The analysing powers for  $\pi^0$  production are positive for both deuteron and proton and of similar size. For  $\pi^-$  production, only

the deuteron data suggest an asymmetry different from zero. The result for  $K^+$  production on the deuteron is compatible with that of  $\pi^+$  production, which may indicate the dominant contribution from  $u$ -quarks fragmenting into kaons.

The results for the two targets show a similar behaviour in their kinematic dependences on  $x$ ,  $P_{\perp}$  and  $z$ . The observed increase of  $A_{\text{UL}}^{\sin\phi}$  with increasing  $x$  suggests that the single-spin asymmetries are associated with valence quark contributions.

Two mechanisms have been proposed to explain the measured single-spin asymmetries. One is the combination of transversity-related chiral-odd distribution functions and chiral-odd fragmentation functions like the Collins fragmentation function. The other one is a final-state interaction of the struck quark with the target remnant (Sivers Effect) [23, 26]. There are no calculations available for the latter scenario that can be compared with the data.

Recent model calculations in the context of transversity [21, 22] predict  $A_{\text{UL}}^{\sin\phi}$  for scattering on the deuteron within the kinematic range of the HERMES experiment. The transversity distributions calculated in the chiral quark soliton model ( $\chi$ QSM) [22], in the SU(6) quark spectator diquark model [21] and in a perturbative QCD model [21] have been used as an input. The results of three of these calculations are displayed in Fig. 6 together with the experimental data. As can be seen from Fig. 6, the experimental data are well described by these calculations.

The dependence of  $A_{\text{UL}}^{\sin 2\phi}$  on  $x$  is presented in Fig. 7. Integrated over the measured  $x$ -range, it is compatible with zero for all mesons (see Tab. I). Also shown are the analysing powers  $A_{\text{UL}}^{\sin 2\phi}$  calculated in the  $\chi$ QSM [22]. However, the data do not show a trend towards the predicted negative asymmetry for pions at large  $x$ .

The data presented so far are evaluated in the semi-inclusive kinematic range  $0.2 < z < 0.7$ . In Fig. 8, the  $z$ -dependencies of the single spin asymmetries  $A_{\text{UL}}^{\sin\phi}$  on the proton and on the deuteron are shown up to  $z = 1$ . The results on the proton have been obtained from experimental data taken with a longitudinally polarised hydrogen target as described in Ref. [2], neglecting the upper  $z < 0.7$  cut, however. The mean experimental resolution in  $z$  is  $\Delta z = 0.02$  (0.04) for charged (neutral) pions in the semi-inclusive regime and  $\Delta z = 0.07$  (0.06) for  $z \rightarrow 1$ . It has to be pointed out that the experimental data shown as open symbols in Fig. 8 have not been corrected for this variation in  $\Delta z$ . Also, the results for charged pions have not been corrected for a possible contamination by pions from the decay of exclusively produced  $\rho^0$  vector mesons.

At large  $z$ , a transition from the semi-inclusive regime to the exclusive regime is observed. In the exclusive limit ( $z \rightarrow 1$ ), the scattering process can be interpreted in terms of generalised parton distributions [38, 39, 40, 41]. The data show an inversion of the sign and an increase

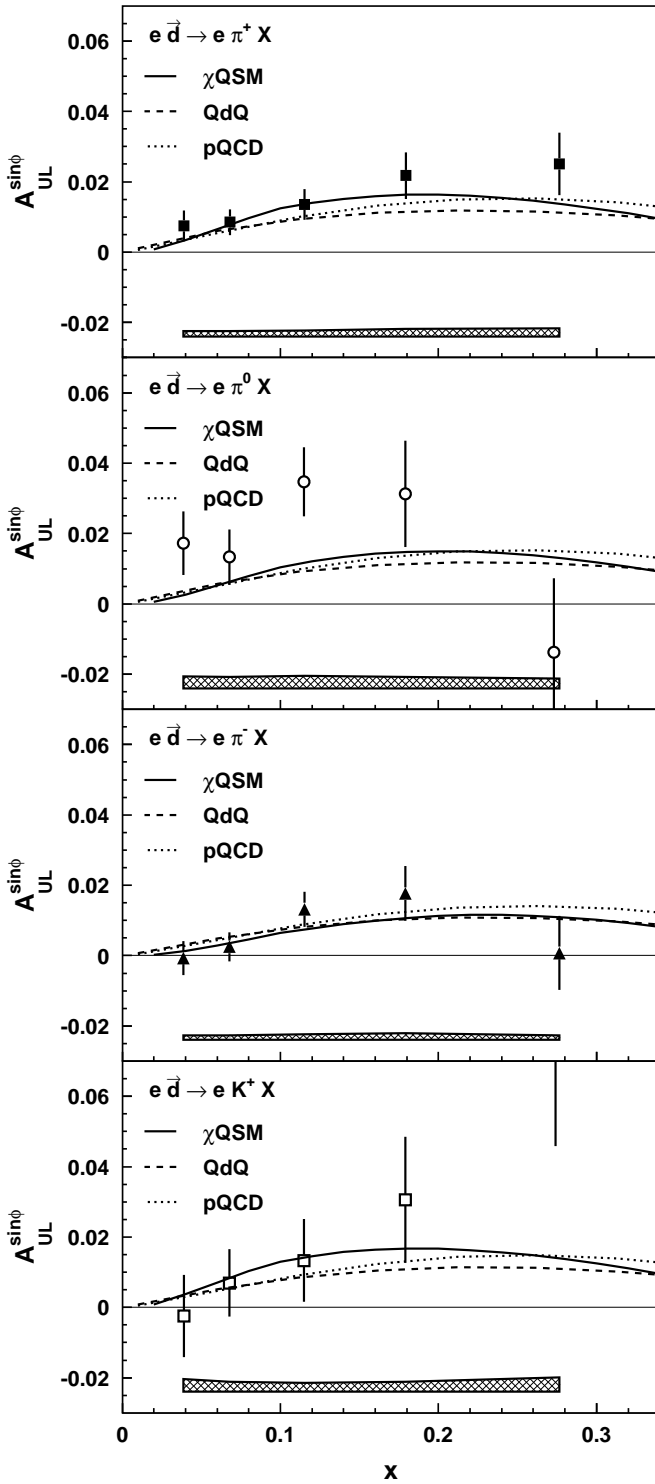


FIG. 6: Comparison of the measured analysing powers  $A_{UL}^{\sin\phi}$  on the deuteron for  $\pi^+$ ,  $\pi^0$ ,  $\pi^-$  and  $K^+$  production with predictions from theoretical calculations in the chiral quark soliton model ( $\chi$ QSM, *solid lines* [22]), the quark-diquark model (QdQ, *dashed lines* [21]) and a perturbative QCD model (pQCD, *dotted lines* [21]). The shown curves refer to “approach 2” of the models in Ref. [21]. The error bars give the statistical uncertainties of the measurements, the bands in the lower part of the panels show the systematic uncertainties of the measurements.

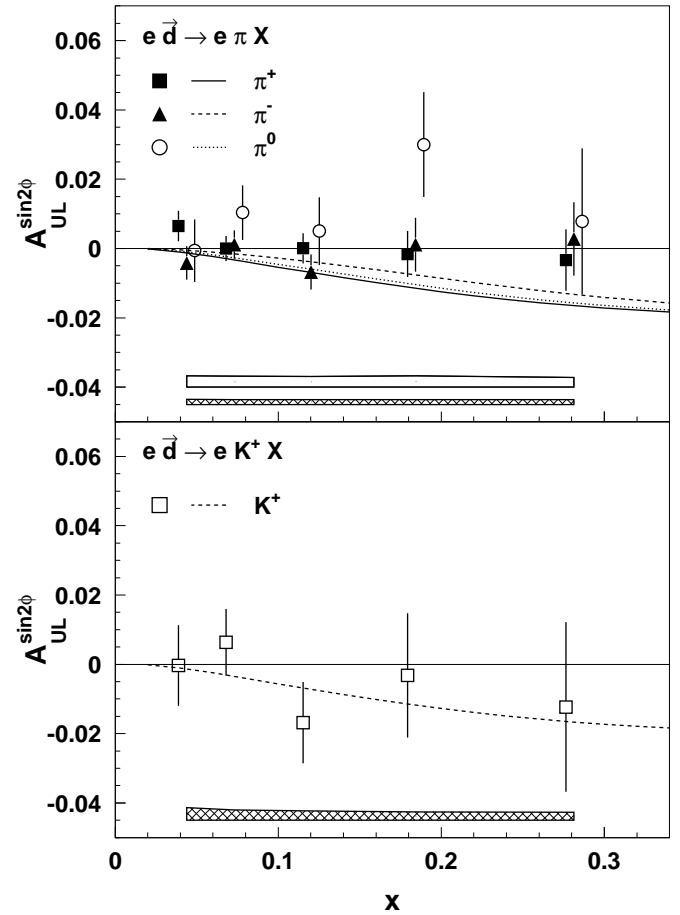


FIG. 7: The  $\sin 2\phi$  analysing powers  $A_{UL}^{\sin 2\phi}$  for  $\pi^+$ ,  $\pi^0$  and  $\pi^-$  (*upper panel*) and for  $K^+$  production (*lower panel*) on the deuteron. The error bars give the statistical uncertainties of the measurements. The systematic uncertainties for  $\pi^+$  and  $\pi^-$  are represented by the hatched band and those for  $\pi^0$  by the open band. The points for  $\pi^0$  and  $\pi^-$  are slightly shifted in  $x$  for better visibility. Included as curves are predictions from a transversity-related calculation in the chiral quark soliton model [22].

in absolute size of the single spin asymmetries, similar for both  $\pi^-$  and  $\pi^+$ . The size of the asymmetry for  $\pi^0$  mesons increases but it remains positive for all  $z$ . A large asymmetry in the exclusive limit has already been reported for exclusive  $\pi^+$  production on the proton [42]. As shown in the lower panel of Fig. 8, there is a large analysing power for  $\pi^0$  production on the proton as well, while no significant asymmetry for  $\pi^-$  production is found. No theoretical explanation yet exists for this experimental result.

In summary, single-spin azimuthal asymmetries for electroproduction of  $\pi^+$ ,  $\pi^0$ ,  $\pi^-$  and  $K^+$  mesons on a longitudinally polarised deuterium target have been measured for the first time. The dependences of these asymmetries on  $x$ ,  $P_\perp$  and  $z$  have been investigated. The results show positive asymmetries for  $\pi^+$  and  $\pi^0$  and an indication of a positive asymmetry for  $\pi^-$  mesons.

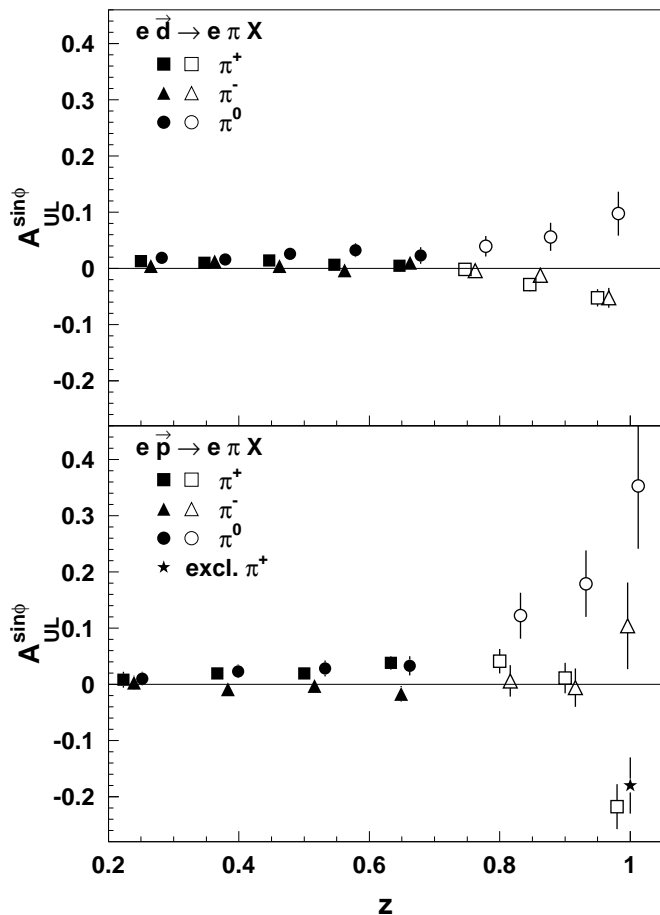


FIG. 8: The dependence on  $z$  of the analysing powers  $A_{UL}^{\sin\phi}(z)$  for  $\pi^+$ ,  $\pi^0$  and  $\pi^-$  production on the deuteron (*upper panel*) and on the proton (*lower panel*). The filled symbols show the semi-inclusive measurements on the deuteron from Fig. 5 and on the proton from Ref. [2], respectively. Shown as filled star is the exclusive measurement for  $\pi^+$  production from Ref. [42]. For the data at high  $z$  (*open symbols*), no corrections for the experimental resolution in  $z$  or possible contaminations by pions from the decay of exclusive  $\rho^0$  vector mesons have been applied. The error bars indicate the statistical uncertainty of the measurements. The points for  $\pi^0$  and  $\pi^-$  are slightly shifted in  $z$  for visibility.

The asymmetry for  $K^+$  is compatible with that for  $\pi^+$  mesons. These findings can be well described by model calculations where the asymmetries are interpreted in the context of transversity as the effect of combinations of chiral-odd distribution functions and chiral-odd fragmentation functions. Here, the observed asymmetries for  $\pi^+$  and  $K^+$  are consistent with the assumption of  $u$ -quark dominance in the quark distribution and the fragmentation process. Together with earlier measurements on the proton [2, 3], the results support the existence of non-zero chiral-odd distribution functions that describe the transverse polarisation of quarks. However, it cannot be excluded that a part of the observed asymmetry is due to an additional exchange of a gluon in the final state

(Sivers effect) as discussed in Ref. [23]<sup>1</sup>. Furthermore, the data show an increase of the magnitude of the asymmetries for charged and neutral pions at large  $z$  when approaching the exclusive regime.

We thank M. Anselmino, A. Bachtetta, A.M. Kotzinian, P.J. Mulders and P. Schweitzer for many interesting discussions on this subject. We gratefully acknowledge the DESY management for its support, the staffs at DESY and the collaborating institutions for their significant effort. This work was supported by the FWO-Flanders, Belgium; the Natural Sciences and Engineering Research Council of Canada; the ESOP, INTAS and TMR network contributions from the European Union; the German Bundesministerium für Bildung und Forschung; the Italian Istituto Nazionale di Fisica Nucleare (INFN); Monbusho International Scientific Research Program, JSPS and Toray Science Foundation of Japan; the Dutch Foundation for Fundamenteel Onderzoek der Materie (FOM); the U.K. Particle Physics and Astronomy Research Council; and the U.S. Department of Energy and National Science Foundation.

- 
- [1] P.J. Mulders and R.D. Tangerman, Nucl. Phys. B **461**, 197 (1996) and Nucl. Phys. B **484**, 538 (1997) Erratum.
  - [2] HERMES Collaboration, A. Airapetian *et al.*, Phys. Rev. Lett. **84**, 4047 (2000).
  - [3] HERMES Collaboration, A. Airapetian *et al.*, Phys. Rev. D **64**, 097101 (2001).
  - [4] A. Bravar for the SMC Collaboration, Nucl. Phys. B (Proc. Suppl.) **79**, 520 (1999).
  - [5] J. Collins, Nucl. Phys. B **396**, 161 (1993).
  - [6] J.D. Ralston and D.E. Soper, Nucl. Phys. B **152**, 109 (1979).
  - [7] X. Artru, M. Mekhfi, Z. Phys. C **45**, 669 (1990).
  - [8] R.L. Jaffe and X. Ji, Phys. Rev. Lett. **67**, 552 (1991) and Nucl. Phys. B **375**, 527 (1992).
  - [9] A.M. Kotzinian, Nucl. Phys. B **441**, 234 (1995).
  - [10] P.J. Mulders, Nucl. Phys. A **622**, 239c (1997).
  - [11] K.A. Oganessyan, H.R. Avakian, N. Bianchi and A.M. Kotzinian, Proc. of BARYONS'98, 320 (1998); hep-ph/9808368.
  - [12] D. Boer, RIKEN Rev. **28**, 26 (2000); hep-ph/9912311.
  - [13] M. Boglione and P.J. Mulders, Phys. Lett. B **478**, 114 (2000).
  - [14] A.V. Efremov, K. Goeke, M.V. Polyakov and D. Urbano, Phys. Lett. B **478**, 94 (2000).
  - [15] E. De Sanctis, W.-D. Nowak and K.A. Oganessyan, Phys. Lett. B **483**, 69 (2000).

---

<sup>1</sup> New data are expected from HERMES measurements on a transversely polarised target, which will be able to distinguish between the two possible causes of these single-spin asymmetries — the combination of transversity with the Collins fragmentation function, or the Sivers Effect [25].

- [16] M. Anselmino and F. Murgia, Phys. Lett. B **483**, 74 (2000).
- [17] A.M. Kotzinian, K.A. Oganessyan, H.R. Avakian and E. De Sanctis, Nucl. Phys. A **666-667**, 290c (2000).
- [18] K.A. Oganessyan, N. Bianchi, E. De Sanctis, W.-D. Nowak, Nucl. Phys. A **689**, 784 (2001).
- [19] B. Ma, I. Schmidt and J. Yang, Phys. Rev. D **63**, 037501 (2001).
- [20] A.V. Efremov, K. Goeke, M.V. Polyakov and D. Urbano, Phys. Lett. B **522**, 37 (2001) and Erratum Phys. Lett. B **544**, 389 (2002).
- [21] B. Ma, I. Schmidt and J. Yang, Phys. Rev. D **66**, 094001 (2002).
- [22] A.V. Efremov, K. Goeke, P. Schweitzer, Eur. Phys. J. C **24**, 407 (2002).
- [23] S. Brodsky, D. Hwang and I. Schmidt, Phys. Lett. B **530**, 99 (2002).
- [24] J. Collins, Phys. Lett. B **536**, 43 (2002).
- [25] D.W. Sivers, Phys. Rev. D **41**, 83 (1990) and Phys. Rev. D **43**, 261 (1991).
- [26] X. Ji and F. Yuan, Phys. Lett. B **543**, 66 (2002).
- [27] M. Anselmino, M. Boglione and F. Murgia, Phys. Lett. B **362**, 164 (1995).
- [28] D. Boer and P.J. Mulders, Phys. Rev. D **57**, 5780 (1998).
- [29] M. Boglione and P.J. Mulders, Phys. Rev. D **60**, 054007 (1999).
- [30] V. Korotkov, W.-D. Nowak and K. Oganessyan, Eur. Phys. J. C **18**, 639 (2001).
- [31] A. Sokolov and I. Ternov, Sov. Phys. Doklady **8**, 1203 (1964).
- [32] D.P. Barber *et al.*, Phys. Lett. B **343**, 436 (1995).
- [33] D.P. Barber *et al.*, Nucl. Instrum. Methods A **329**, 79 (1993).
- [34] M. Beckmann *et al.*, Nucl. Instrum. Methods A **479**, 334 (2002).
- [35] HERMES Collaboration, K. Ackerstaff *et al.*, Nucl. Instrum. Methods A **417**, 230 (1998).
- [36] N. Akopov *et al.*, Nucl. Instrum. Methods A **479**, 511 (2002).
- [37] H. Avakian *et al.*, Nucl. Instrum. Methods A **417**, 69 (1998).
- [38] D. Müller, D. Robaschik, B. Geyer, F.-M. Dittes and J. Horejsi, Fortschr. Phys. **42**, 101 (1994).
- [39] A.V. Radyushkin, Phys. Rev. D **56**, 5524 (1997).
- [40] L.L. Frankfurt, P.V. Polyakov, M. Strikman and M. Vanderhaeghen, Phys. Rev. Lett. **84**, 2589 (2000).
- [41] A.V. Belitsky and D. Müller, Phys. Lett. B **513**, 349 (2001).
- [42] HERMES Collaboration, A. Airapetian *et al.*, Phys. Lett. B **535**, 85 (2002).